ACS Catalysis

pubs.acs.org/acscatalysis

Research Article

Electrochemical Manufacturing of Hydrogen Peroxide with High Concentration and Durability

Yang Xia, Peng Zhu, Yile Yang, Chang Qiu, and Haotian Wang*

Cite This: ACS Catal. 2025, 15, 4560−4569

Read Online

ACCESS | Metrics & More | Article Recommendations | Supporting Information

ABSTRACT: Electrochemical manufacturing of hydrogen peroxide (H_2O_2) via oxygen reduction reaction (ORR) has been widely recognized as an alternative to the conventional anthraquinone process, but the output H_2O_2 concentration that it can reach and the long-term electrolysis stability are still far from industrial requirements. Here, we report the promising potential of the porous solid electrolyte (PSE) reactor for producing high-concentration and high-purity H_2O_2 in high stability. By identifying the issue of high H_2O_2 concentration at the cathode/membrane interface that could lead to membrane degradation and low ORR Faradaic efficiencies (FEs), we adopted a water recirculation flow operation instead of continuous flow to effectively carry out the generated H_2O_2 product from the PSE layer without interfacial accumulation. This recirculation strategy boosted the H_2O_2 FE from 23% to 50% to produce a 30 wt % H_2O_2 stream and successfully extended the lifetime of the PSE reactor to ∼1000 h while continuously outputting 20 wt % H_2O_2 under 100 mA cm^{-2} operation current.

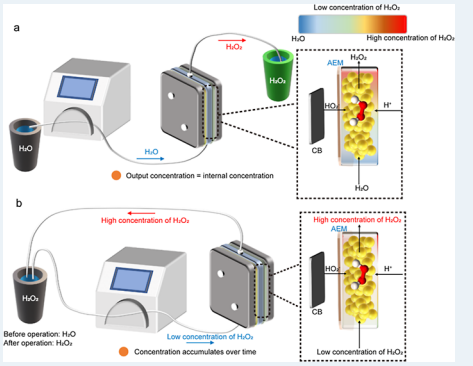

KEYWORDS: *electrocatalysis, hydrogen peroxide, oxygen reduction reaction, ultrahigh concentration, improved lifetime*

INTRODUCTION

Hydrogen peroxide (H_2O_2) is one of the most crucial and fundamental chemicals due to its wide applications in different industries, including paper and pulp manufacturing, disinfection, wastewater treatment, chemical synthesis, etc.[1−3] The incumbent industrial method for large-scale H_2O_2 production is the anthraquinone cycling process, which is a traditional chemical process based on the hydrogenation of 2-alkyl-9/10-anthraquinone with H_2 followed by subsequent oxidation with O_2 in an organic solvent (Figure 1a).[4] This long-established traditional method can realize large-scale production of H_2O_2 with high concentrations (tens of percent by weight). However, this process consumes significant amounts of H_2 from fossil fuels and generates a large amount of CO_2 emission (∼3 tons of CO_2 emission per ton of H_2O_2 produced).[5,6] The fabrication process also involves organic molecules and solvents, producing a large quantity of organic waste.[2,7] Moreover, the process typically needs centralized large infrastructure to become economically viable, which necessitates the transportation and storage of highly concentrated H_2O_2 solutions that are hazardous to handle. Alternative strategies to synthesize H_2O_2, with less energy consumption, waste, production cost, and safety issues, are highly desired, especially when carbon neutralization is becoming increasingly emphasized globally nowadays.

Electrochemical synthesis of H_2O_2 from oxygen reduction reaction (ORR) via a $2e^-$ transfer process has attracted intensive interest from both academia and industry in recent years (Figure 1b).[8−13] Compared to the traditional anthraquinone process, its advantages include mild reaction conditions under ambient temperature, renewable electricity input (from solar panels, wind turbines, etc.) without CO_2 emissions, and high-energy conversion efficiencies, as well as sustainable input feedstocks such as air and water. It can realize decentralized production of H_2O_2 compared to the traditional method, therefore avoiding the concentration−transportation−dilution process in many applications where low-concentration H_2O_2 is typically used. Instead of producing H_2O_2 chemically via the organic chemistry route, the electrochemical approach reduces O_2 to generate H_2O_2 with the energy input of electricity that could come from renewable sources. However, there are still significant challenges preventing the electrochemical synthesis of H_2O_2 from large-scale deployments. For example, in traditional H_2O_2 electrolyzers, liquid electrolytes are typically used to serve both efficient ion conduction for high energy efficiencies and H_2O_2 collection. Thus, one intrinsic burden for this technique to be scaled up economically is its ionic impurities mixed in the H_2O_2 product solution, such as K^+, Na^+, SO_4^{2-}, etc.[11−15] Similar to the produced H_2O_2 in the industrial anthraquinone process, those as-generated H_2O_2 solutions from electrolyzers need an extra

Received: November 14, 2024
Revised: February 18, 2025
Accepted: February 19, 2025

https://doi.org/10.1021/acscatal.4c07033
ACS Catal. 2025, 15, 4560−4569

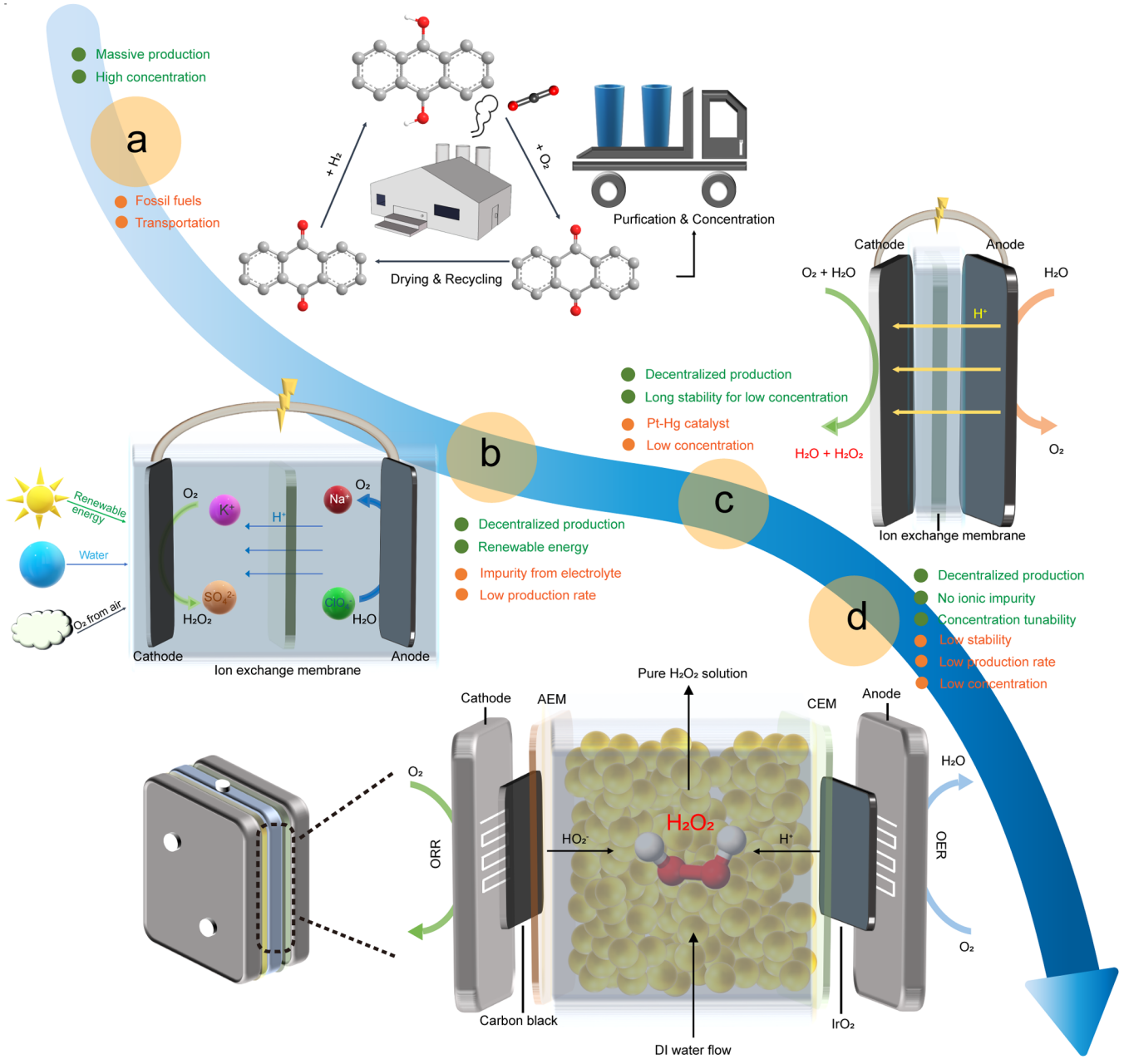

Figure 1. Schematics of different methods of H_2O_2 production. (a) Industrial anthraquinone process, (b) traditional electrochemical method, (c) proton-exchange membrane MEA method, and (d) our previously reported porous solid electrolyte (PSE) reactor method.

separation process to remove those ionic impurities before being used in practical applications, which leads to high energy consumptions, high costs, and also complicates the technology's decentralized deployments.[16−18] This H_2O_2 product mixture with liquid electrolyte was considered one of the major technical barriers that prevented the electrochemical approach from being commercialized on a large scale.

Replacing the liquid electrolyte with polymer electrolytes, such as ion-exchange membranes, in a typical membrane electrode assembly (MEA) device could avoid these ionic impurities while maintaining low cell resistances for high energy efficiencies.[19] One representative example is using a proton-exchange membrane (PEM) for acidic H_2O_2 generation (Figure 1c).[20,21] The cathode and anode were separated by a PEM, and the protons generated at the anode via the oxygen evolution reaction were transported through the cation-exchange membrane (CEM) to couple with O_2 and electrons at the cathode side via $2e^-$ ORR to form H_2O_2. However, due to the strong acidic environment at the ORR interface, this PEM reactor design presents several disadvantages that could hinder it from being used in large-scale practical applications. First, different from an alkaline environment where low-cost catalysts such as carbon-based materials are present, the catalyst used in this setup usually involves expensive noble metals and potentially harmful metal elements, e.g., Pt−Hg.[10,22] Furthermore, the product concentration this method can achieve was relatively low (~1 wt %) due to further reductions of H_2O_2 to H_2O at this strong acidic interface.[23] While an anion-exchange membrane (AEM) MEA design can avoid noble metal catalysts or further reductions by creating an alkaline reaction interface, its limitation lies in the crossover oxidation of generated HO_2^- back to the anode side to O_2.

https://doi.org/10.1021/acscatal.4c07033
ACS Catal. 2025, 15, 4560−4569

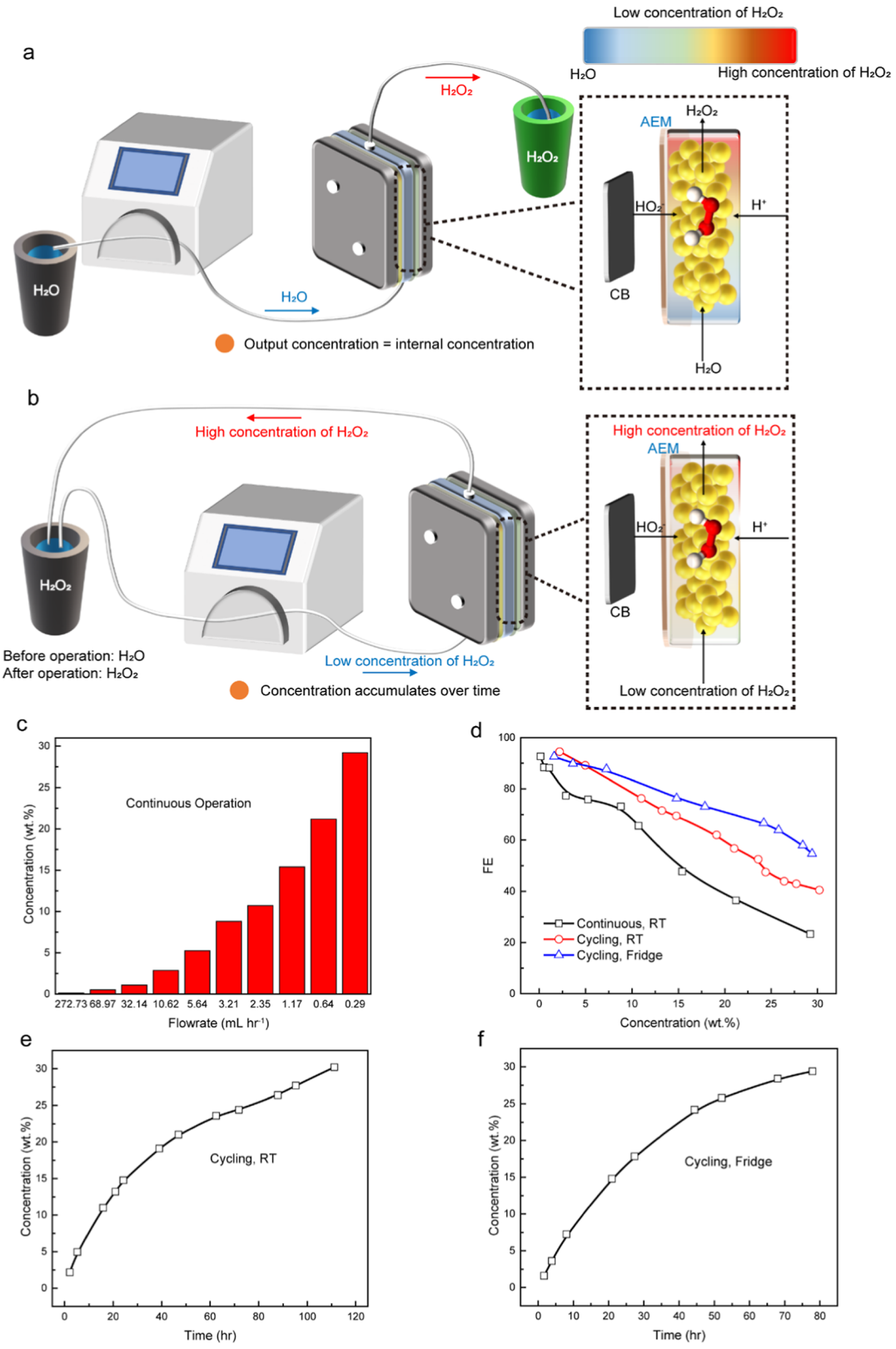

Figure 2. Continuous flow and water recirculation flow methods of H_2O_2 production. (a) Continuous flow schematics; (b) water recirculation flow schematics; (c) product H_2O_2 concentration as a function of the water-carrying flow rate for the continuous-flow method; (d) comparison of FE of different target product concentrations for three different operation conditions: continuous flow under room temperature (black), water recirculation flow under room temperature (red), and water recirculation flow under low temperature (blue), respectively; and (e,f) concentration vs time for water recirculation flow schematics under room temperature and low temperature, respectively.

Our group previously reported a three-chamber PSE reactor design to address the challenges mentioned above for direct and continuous electrochemical synthesis of high-purity H_2O_2 solutions.[24] Instead of using traditional liquid electrolytes,

https://doi.org/10.1021/acscatal.4c07033
ACS Catal. 2025, 15, 4560−4569

porous solid electrolytes were used solely for the function of ionic conduction, while pure DI water stream was supplied for product collection (Figure 1d). The use of solid electrolyte is crucial since it can offer good conductivity with small ohmic loss as well as promote the recombination of HO_2^- and H^+ and introduce no ion impurity compared to the cases of traditional cell configurations. Product concentrations can be effectively tuned by controlling the DI water flow rate. With this configuration, decentralized H_2O_2 production can be realized without involving ionic impurities, and the product concentration can be precisely tuned and controlled to meet the requirements in different application scenarios. However, there are still several challenges that need to be addressed with this technology. First, in previous studies, we have reached a maximum of 200 h of stability using a B−C catalyst in this solid-electrolyte setup.[25] However, industrial applications require thousands of hours of stability for economical production. Thus, the current operation stability is still below the industrial requirements. Furthermore, the previous long-term stability tests that we performed were under relatively low current densities, which suggests high capital costs in real applications. In general, electrochemical applications need at least 100 mA cm^{-2} current density operation to guarantee a low capital cost to reach competitive production cost compared to traditional approaches. Last but not least, the H_2O_2 concentration that has been demonstrated in stability tests so far was still not high enough. In our previous works, most stability concentrations ranged from thousands of ppm to 1−2 wt %, which is enough in most disinfection processes. However, for many other applications like paper and pulp industry and chemical synthesis, tens of weight percent level (20−30 wt %) of H_2O_2 is typically used. Additionally, the H_2O_2 Faradaic efficiency (FE) when reaching ultrahigh concentration becomes much lower than low concentration.[24,26] Specifically, when the H_2O_2 product concentration was increased from 3 wt % to 20 wt %, the selectivity dropped from 90% to only ∼20% as reported in our previous work.[24] This significant degradation in selectivity possibly happened due to several reasons: (1) the H_2O_2 crossover, where the as-generated ultrahigh concentration of H_2O_2 can undergo crossover to the anode side through CEM via diffusion and permeation; (2) the self-decomposition, as ultrahigh concentration of H_2O_2 is not stable under high temperature or strong light conditions; and (3) reverse reaction and overreduction. Thus, how to produce high concentrations of H_2O_2 solutions for industrially relevant stable periods (thousands of hours) under practical current densities is still a big challenge. Here, we demonstrate the practical operation of electrochemical H_2O_2 synthesis in our solid electrolyte reactor. We showed that the catalyst/electrolyte interface presents high concentrations of H_2O_2 that cause low FEs and poor stability. By changing the continuous water flow mode to a recirculation mode in the PSE layer, we were able to deliver a highly stable generation (∼1000 h) of high-concentration H_2O_2 solutions (20 wt %) under a current density of 100 mA cm^{-2} while maintaining a high FE of over 60%.

RESULTS AND DISCUSSION

In the case of continuous flow of DI water through the PSE layer as reported in our previous work (4 cm^2 electrode),[24] when ultrahigh concentration of H_2O_2 (such as 20 wt %) was targeted, the DI water flow rate needs to be reduced to extremely slow, from 16.2 mL h^{-1} to 0.5 mL h^{-1} (by a factor of 32.4) under a fixed ORR current density of 100 mA cm^{-2}. This significant drop in the flow rate can cause a series of negative impacts on the reactor system performance, especially in terms of the self-decomposition reaction of H_2O_2 (eq 1)

$$2H_2O_2(aq) \rightarrow 2H_2O(l) + O_2(g) + \text{heat} \quad (1)$$

When an ultrahigh concentration of H_2O_2 is produced, the significant amount of heat and bubbles generated at the interface could harm the membrane stability.[27,28] Additionally, when the flow rate is extremely low, the accumulative HO_2^- concentration at the membrane−solid electrolyte interface becomes exceptionally high. This will cause several problems: first, the extremely high concentration of HO_2^- remaining at the interface might do harm to the membrane stability due to its oxidation capability; moreover, the high concentration of HO_2^- cannot be transported efficiently, making the undesired reverse reaction, self-decomposition, and crossover more easily to happen, further decreasing the selectivity. Increasing the water flow rate could enhance the diffusion of HO_2^- away from the interface, improving the reaction stability and H_2O_2 selectivity. However, a high DI water flow rate inevitably results in a low product concentration in continuous flow operation mode. Thus, we propose to change the continuous operation mode to a batch synthesis by recirculating a fixed amount of DI water through the PSE layer during a certain period for H_2O_2 accumulation.

As shown in Figure 2a, in the previous continuous reaction scheme, pure water is fed into the reactor and the H_2O_2 product is directly collected at the outlet stream. Thus, the outlet product H_2O_2 concentration is the same as the internal concentration inside the reactor. To meet the requirement for ultrahigh concentration for the outlet stream, the flow rate must be kept to an extremely low value. This will cause low stability and low selectivity problems vide ante. Instead of a continuing flow to collect a specific volume of highly concentrated H_2O_2 solution within a certain period, recirculating a fixed volume of DI water, which is the same as the final volume of the continuous flow mode, for the same period could effectively lower the average H_2O_2 concentration with which the membrane and PSE layer of our reactor are in contact with. As shown in Figure 2b, before the reaction process, the product collection bath is filled with a certain volume of pure water. When the reaction begins, a low concentration of H_2O_2 is produced and collected in the outlet stream. Instead of being collected in another product container in the continuous-flow scheme, the product stream is recirculated back into the initial feeding container. In this case, the water flow rate can be tuned relatively high. In our test, we used 4.5 mL min^{-1}, which is about 420 times quicker than the case in the continuous flow mode for a product concentration of 20 wt %. At the start of the experiment, the initial concentration is zero (or pure water). The concentration will build up as the experiment proceeds, given the fixed cycling volume. Given this improved reaction scheme, we assume that the local H_2O_2 concentration at the AEM/PSE interface will decrease, and the FE of H_2O_2 will increase due to lower interfacial concentration and higher water carry-out rate.

To demonstrate the advantages of the recirculation operation mode, we started with a BP2000 carbon black catalyst coated on a 6.25 cm^2 electrode as the $2e^-$-ORR cathode (see Matierials and Methods), due to its commercial availability, high surface area, and good H_2O_2 activity and selectivity (Figures S1−S3). To avoid the required flow rate falling below the operational limit of the water pump in continuous flow mode (while aiming for 30 wt % concentration), the electrode area was designed to be larger than our standard 4 cm^2 configuration. First, we

https://doi.org/10.1021/acscatal.4c07033
ACS Catal. 2025, 15, 4560−4569

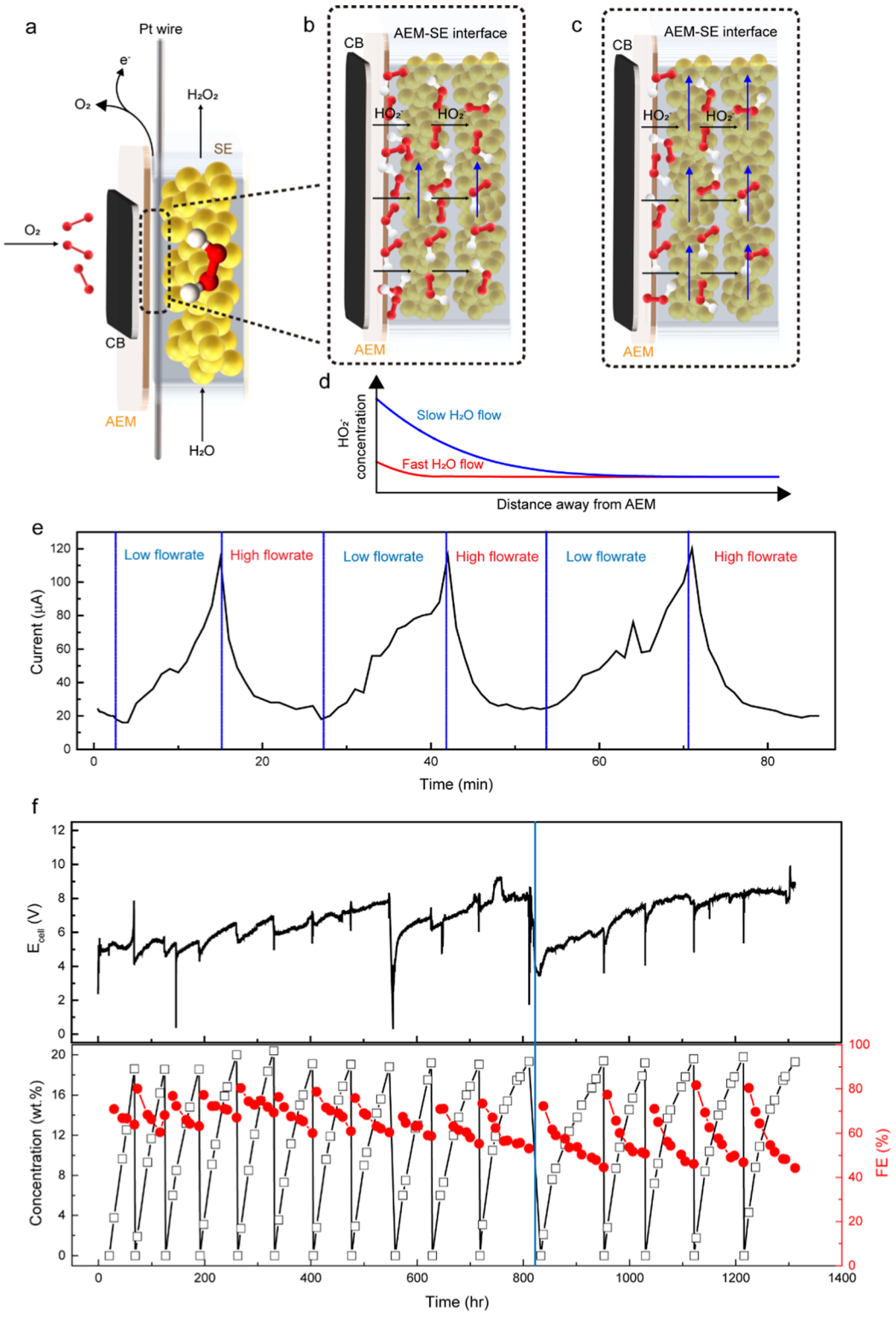

Figure 3. Local HO_2^- concentration and stability demonstration for continuous flow and water recirculation flow operations of H_2O_2 production. (a) Schematics of interfacial concentration measurement with the help of a Pt wire. (b,c) Concentration gradient and diffusion schematics of low and high interfacial flow rates, respectively. (d) Concentration profile at the AEM/PSE interface from COMSOL. (e) H_2O_2 oxidation current detected as a function of time. Note that the flow rate was alternated between low and high values. The blue vertical lines indicate the time when the flow rate was switched. (f) Long-term operation of generating 20 wt % pure H_2O_2 solutions using the water recirculation operation mode. The voltage over time (upper panel) and the corresponding concentration and FE over time (lower panel) were plotted, respectively. The cell voltage was not *iR* compensated. Note that the blue vertical line indicates a mechanical failure (rupture) of the AEM.

operated the PSE reactor in a continuous flow operation mode, as shown in the schematics described in Figures 1d and 2a, under room temperature. The cell current density was fixed at 100 mA cm^{-2}, with an overall cell current of 625 mA. The DI water flow

https://doi.org/10.1021/acscatal.4c07033
ACS Catal. 2025, 15, 4560−4569

rate was initially set at 4.55 mL min^{-1} and gradually decreased to increase the output H_2O_2 concentration. Please note here that while the liquid flow rate into and out of the PSE layer was quite similar when the DI water flow rate was high, the output flow rate could be significantly deviated from the input under low DI water flow rates due to the generation of H_2O_2 as well as osmosis effects. Therefore, all of the liquid flow rates recorded in this study were calibrated at the output. The product concentration and H_2O_2 FE were determined by the titration method (see Materials and Methods). Figure 2c shows the output H_2O_2 concentrations as a function of the liquid flow rate, with a maximal concentration of ~30 wt % reached at a flow rate of 0.0048 mL min^{-1}. Note that the density deviation of the output H_2O_2 solution from pure water was considered when the H_2O_2 concentration was calculated. As the H_2O_2 concentration increased, we noticed that its FE continued to drop, as shown in Figure 2d. Specifically, from the black curve, the H_2O_2 FE was high (over 85%) for the low concentration range, which is consistent with the results that we reported previously (less than 3 wt %).[24,25] When the concentration reached higher values, the FE started to decrease. At an ultrahigh H_2O_2 concentration of 30 wt %, which is the most commonly commercially available bulk H_2O_2 concentration, the FE dropped to only about 23%. Under the same testing conditions (same current density and electrode size), the recirculation flow mode was also operated for a direct performance comparison, during which the liquid recirculation flow rate was fixed at 4.5 mL min^{-1}. The product concentrations and FEs were sampled at different times during batch operation (Figure 2e). Please note here that the total middle layer liquid volume could increase over time due to osmosis effects, which was also considered in the FE calculation. Compared with the continuous flow scheme, the H_2O_2 FE also decreased with the increasing concentration. This trend itself is reasonable since the H_2O_2 self-decomposition and crossover rate increase with increasing H_2O_2 concentration. However, the H_2O_2 FE at higher concentrations significantly improved compared with the continuous flow operation mode. At 30 wt % concentration, the FE under recirculation mode was over 40% (the red curve on Figure 2d), almost 20% higher than the continuous-flow case. This result supports our proposition that a lower interfacial concentration and higher flow rate can suppress the H_2O_2 self-decomposition and crossover rate. To further support this point, we operated the electrolysis under a lower temperature (~10 °C) where the H_2O_2 self-decomposition rate and crossover rate can be further brought down but at a sacrifice of reaction activity (higher cell voltage). Similar to the room-temperature recirculation operation, the concentrations and FEs were determined at different times after the start of electrolysis (Figure 2f). As a result, the H_2O_2 FE was further improved to about 50% when delivering 30 wt % H_2O_2 products (the blue curve on Figure 2d), representing the benchmark performance of electrochemical synthesis of H_2O_2 in the literature to the best of our knowledge.

While our hypothesis is that the different interfacial H_2O_2 concentrations under continuous flow and recirculation mode are responsible for the different H_2O_2 FE performances under high concentrations, we still do not have direct evidence. Inspired by the working mechanism of rotating ring-disc electrode setup, here, we placed a positively biased ultrathin (0.1 mm-diameter) platinum (Pt) wire at the AEM/PSE interface to detect the in situ-generated H_2O_2 (Figure 3a). The oxidation current of H_2O_2 at the Pt wire was monitored to qualitatively assess the concentration of H_2O_2 at the AEM/PSE interface under various operating conditions. The observed oxidation current should provide insight into the local accumulation of HO_2^-, which is influenced by the water flow rate. At higher flow rates, the local accumulation of HO_2^- is reduced, leading to a lower oxidation current. Conversely, at lower flow rates, the increased accumulation of HO_2^- results in a correspondingly higher oxidation current (Figure 3b,c). To further investigate how the interfacial HO_2^- concentration could change with different flow rates, we constructed a two-dimensional (2D) COMSOL model to map out the HO_2^- concentration distribution near the catalyst surface (Figures 3d and S4). Specifically, the simulation was performed under two flow rates: a higher flow rate (4.5 mL min^{-1}) and a lower flow rate (0.27 mL min^{-1}) were tested under an ORR current of 100 mA cm^{-2}. As expected, the HO_2^- concentration is highest at the left-hand boundary, where the reaction occurs and the HO_2^- flux is introduced and reaches a peak near the outlet. Compared to the scenario with the high flow rate, the HO_2^- peak concentration (close to the outlet of the left-hand boundary) is roughly 5 times higher for the low-flow-rate case, while the thickness of the diffusion layer is roughly 4 times thicker. The simulations revealed that higher flow rates result in lower interfacial HO_2^- concentrations and thinner diffusion layers due to enhanced mass transport. Conversely, at lower flow rates, the interfacial HO_2^- concentration increases, accompanied by the formation of a thicker diffusion layer. To examine this relationship experimentally, the water flow rate entering the reactor was systematically varied between a high flow rate (4.5 mL min^{-1}) and a low flow rate (0.27 mL min^{-1}). As shown in Figure 3e, the data indicated that at a higher water flow rate, the local concentration of HO_2^- was reduced, as evidenced by the lower oxidation current measured on the Pt wire surface (20 μA). When the flow rate was decreased to 0.27 mL min^{-1}, the oxidation current increased significantly to 120 μA, reflecting a corresponding rise in the local HO_2^- concentration due to the reduced flow rate. After several minutes, the flow rate was restored to 4.5 mL min^{-1}, resulting in a decrease in the oxidation current. This observed pattern provided direct evidence supporting the proposed inverse relationship between the water flow rate and the interfacial HO_2^- concentration.

Based on this finding, we proposed to tackle the stability challenge using the recirculation flow mode. Even though it significantly improved the H_2O_2 FE when reaching ultrahigh concentrations, whether this mode can be operated stably over thousands of hours, which is necessary for considering industrial-relevant long-term operations, remains uncertain. Following the same experimental setup in Figure 2b, we targeted 20 wt % H_2O_2 concentration since it can satisfy most of the high-concentration application scenarios. In Figure 3f, both concentrations and the FEs were plotted versus the reaction time. The cell was operated under 100 mA cm^{-2} with an electrode area of 4 cm^2. Please note that the cell was flushed with pure DI water between each two cycles to ensure the measured concentration for subsequent cycles was accurate (see Figure S5 and Note S1). The average FE for each cycle remained over 55−60% for the first 800 h of operation. We also observed that the H_2O_2 FE slightly decreased within each operation cycle with an increased H_2O_2 concentration. This might be due to the H_2O_2 self-decomposition, further reductions on the cathode, or crossover oxidation on the anode side. The slight rise in temperature from the increase in cell voltage might also facilitate H_2O_2 degradation, leading to a slight decrease in the FE. Please note that the blue vertical line in Figure 3f corresponds to the

https://doi.org/10.1021/acscatal.4c07033
ACS Catal. 2025, 15, 4560−4569

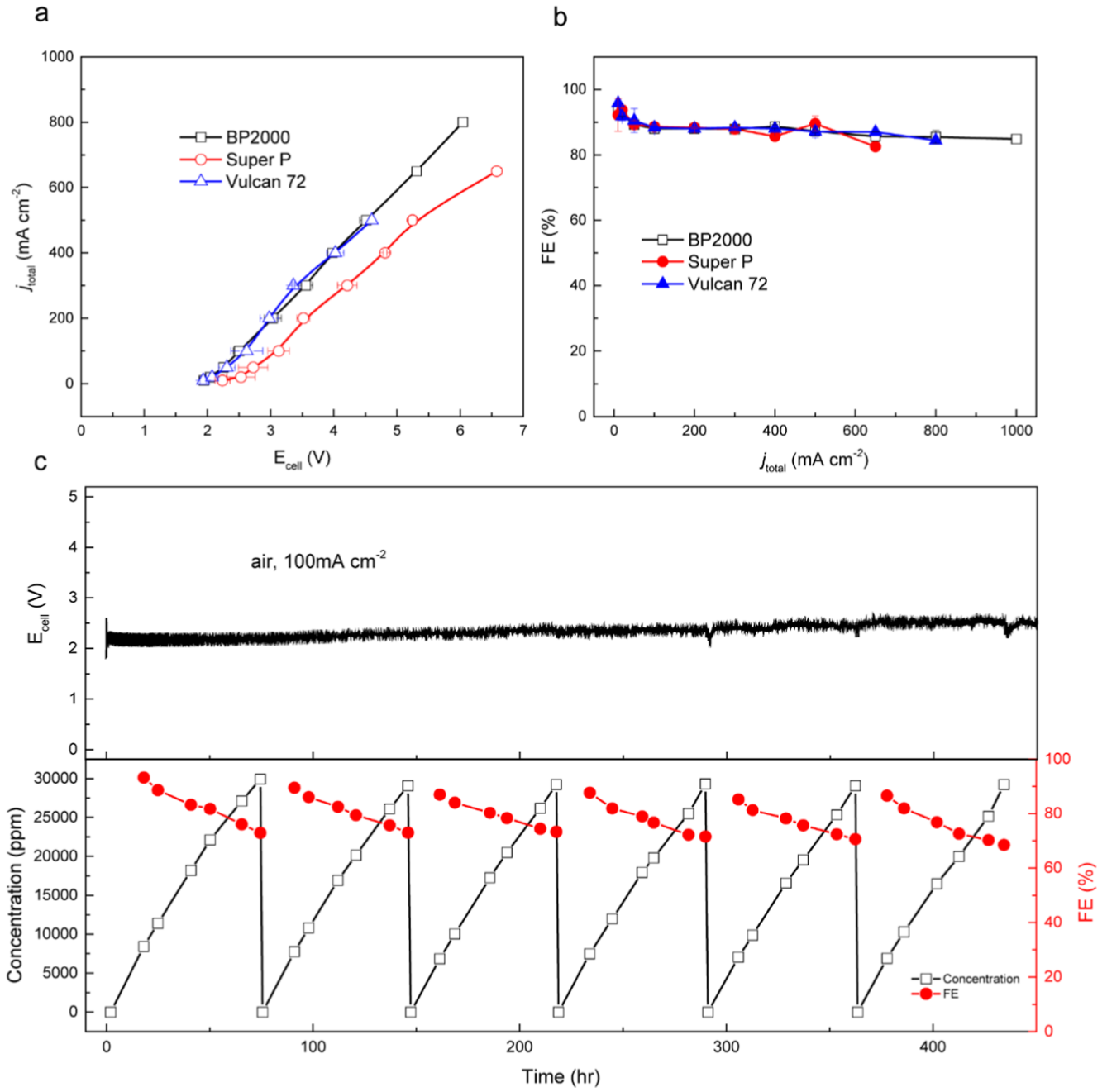

Figure 4. Practical demonstration of H_2O_2 production. (a) Activity of different types of carbon blacks and (b) their corresponding H_2O_2 FEs. Please note that the voltages for BP2000 under 1 A cm^{-2} and for Vulcan 72 under 0.65−0.8 A cm^{-2} were not reported in (a) since they were not stable. (c) Demonstration of the stable ORR test using air for 3 wt % H_2O_2 generation for over 400 h while maintaining over 70% overall FE. Please note that the voltages are not *i*R compensated.

mechanical failure of the AEM (Figure S6). No significant degradation or change in the composition of surface functional groups was confirmed with Fourier-transform infrared (FTIR) spectroscopy (Figure S7). We fixed the problem by switching to a new, intact membrane while keeping other system components (catalyst, solid electrolyte, CEM, and PSE reactor) unchanged. The whole reaction system still managed to run for another 500 h stably. The slight drop in averaged FEs in cycles (55% to 45%) might be due to the catalyst degradation as the new membrane did not improve the FEs. The high-concentration peroxide species could deteriorate some active sites of the catalyst and cluster some particles (see the SEM image in Figure S8) by direct contact because of the mechanical failure of the AEM. Still, the activity did not drop significantly, and the system had a reliable operation of over 1300 h in total. This also provides us with guidance for future AEM designs on its mechanical strength. With the recirculation flow mode, we achieved a stable operation of ∼1000 h, producing a cumulative of 880 mL (Figure S9) of 20 wt % H_2O_2 concentration while maintaining FEs at 50−60%. To the best of our knowledge, this is the best stability reported so far for electrochemical H_2O_2 synthesis under industrial-relevant currents (100 mA cm^{-2}) and high concentrations.

Practical Application Demonstration. With the recirculation flow mode, we performed further tests to show the feasibility of our PSE reactor in more practical deployment

https://doi.org/10.1021/acscatal.4c07033
ACS Catal. 2025, 15, 4560−4569

scenarios. The operation current density is a crucial parameter, as industrially relevant current density (>100 mA cm^{-2}) means low capital cost and smaller carbon footprint of the electrolyzer. Thus, catalytic materials which are already produced on a large scale and can reach high reaction activity and H_2O_2 selectivity are important to future applications. Here, we studied different commercially available carbon black materials including Super P, Vulcan 72, and BP2000, with the surface area ordering from the lowest to the highest.[29,30] In theory, carbon materials with higher surface areas and a greater density of active sites should exhibit enhanced catalytic activity, leading to increased efficiency in reducing energy consumption, while achieving industrially relevant current densities. This is supported by studies[31,32] indicating that the presence of abundant active sites facilitates more effective electron transfer and reaction kinetics, thereby lowering the overpotential required for electrochemical processes. Based on the BET tests (Figure S10), the trend in the surface areas of these three carbon black materials is consistent with the literature reported.[29,30] We compared the performance of these three carbon materials in terms of the highest stable current densities and H_2O_2 FEs. The $I-V$ curves shown in Figure 4a agreed well with the trend of the surface area, with BP2000 delivering the highest stable current density (800 mA cm^{-2}) under the lowest cell voltage (6 V). The H_2O_2 FEs of all three carbon black catalysts were maintained high until there were large current densities. Specifically, BP2000 can still reach a FE of 87% under a high current density of 800 mA cm^{-2}, which suggests great potential for future's commercialization.

The other aspect to consider is the cathode O_2 reactant input in practical scenarios where high-purity O_2 gas is not easily accessible or economically viable. In these cases, it would be more desirable and convenient to directly feed atmospheric air into the reactor for stable H_2O_2 production. As an initial demonstration, we used BP2000 as the catalyst and performed a stability test using air as the cathode feedstock. Please note that we used a 1 cm^2-electrode here to avoid unexpectedly high pressure applied to the system (given that the required air flow rate should be five times of pure O_2). Air from the lab passed through a commercial air filter before it was pumped into the cathode chamber of our reactor. We targeted 3 wt % H_2O_2 concentration as the output product since it is a typical concentration in commercial H_2O_2 products for household uses. From Figure 4c, the system was operated stably for over 400 h without significant degradation in activity or FE. The H_2O_2 selectivity of each bath synthesis cycle remained over 65%−70%. The intrinsic FE after the cell was flushed with pure DI water between each cycle remained stable and high (Figure S11). We obtained a cumulative 670 mL of 3 wt % H_2O_2 solution after 6 cycles over the total span of 400 h operation (Figure S12). Compared to the operation under pure O_2 input, our technology can fully utilize air as the input without significantly sacrificing H_2O_2 selectivity or cell voltage, demonstrating its great potential for future practical applications where pure O_2 is not accessible.

Techno-Economic Analysis. A preliminary techno-economic analysis (TEA) was performed based on the performance of our PSE reactor with air input shown in Figure 4c (see details in Note S2) to assess its economic viability and adaptability. Please note that the TEA was performed based on the experimental and literature data collected in 2022−2023. The assumptions were made based on a scaled-up version of the device following the previously reported methods.[33] The electricity price was assumed to be 7.9 cents kWh^{-1}.[34] The analysis indicates a total system cost of approximately \$1.16 kg^{-1} per pure H_2O_2 produced based on the industry input on our system performance as well as on capital, operational, and feedstock costs before implementing any improvements (Table S3). The primary cost is contributed to by total capital cost (\$0.45 kg^{-1} H_2O_2), chemical input (\$0.12 kg^{-1} H_2O_2), and electricity (\$0.45 kg^{-1} H_2O_2). Other expenses, including daily maintenance, account for approximately 13% of the total capital cost. This will give a profit of approximately \$1175 per ton of 100% H_2O_2 produced with our reactor. Further improvements can be achieved by reducing the cost of the electrolyzer and enhancing the reaction performance, specifically by decreasing the cell voltage and improving the electron efficiencies. Nonetheless, the development of renewable energy technology and improvements in electrolyzers can be leveraged to reduce the production costs in the near future.

CONCLUSIONS

In conclusion, we developed a promising potential of the PSE reactor for efficiently producing high-concentration and high-purity H_2O_2 under industrial-relevant current densities (100 mA cm^{-2}) in high stability. By identifying the issue of high H_2O_2 concentration at the cathode/membrane interface that could lead to membrane degradation and low ORR FEs, we adopted a water recirculation flow operation instead of continuous flow to effectively carry out the generated H_2O_2 product from the PSE layer without interfacial accumulation. This recirculation strategy boosted the H_2O_2 FE from 23% to 50% to produce a 30 wt % H_2O_2 stream, which, to our knowledge, is the highest reported via an electrochemical approach. We have also successfully extended the lifetime of the PSE reactor to ∼1000 h while continuously outputting 20 wt % H_2O_2 under 100 mA cm^{-2} operation current. High current densities (800 mA cm^{-2}) and stable operation using air over 400 h were also demonstrated for more practical cases. This has provided a huge industrial potential for this technology to be utilized in the majority of industrial application scenarios. Future research will be focused on scaling up this PSE reactor for large-scale H_2O_2 production and further improvements in cell design and configurations for better voltages, current densities, and energy efficiencies.

MATERIALS AND METHODS

Catalyst Materials. Commercially available carbon black (Vulcan XC-72, BP2000, Fuel Cell Store, super P, Alfa Aesar) was used as the catalyst material.

Characterizations. All of the characterizations were done at the Shared Equipment Authority at Rice University. The surface morphology was measured by SEM on an FEI Quanta 400 field emission scanning electron microscope. BET surface area analysis was performed using a Quantachrome Autosorb-iQMP/Kr BET Surface Analyzer. FTIR spectroscopy was performed using a Nicolet FTIR Infrared Microscope.

Double-Layer Capacitance Measurement. We conducted cyclic voltammetry (CV) experiments for the measurement of C_{dl} of the electrode under various conditions. The bounds of CV were 0.83 and 1.05 vs RHE, with five cycles of CV performed. The following scan rates were used: 40, 45, 50, 70, and 100 mV s^{-1}.

Cell Performance Evaluation. For the two-electrode solid-electrolyte cell for the electrosynthesis of pure H_2O_2, an AEM and a Nafion 1110 film (Fuel Cell Store) were used for anion and cation exchange, respectively. Around 0.5 mg cm^{-2} of the carbon catalyst and IrO_2 loaded on WS0101 carbon cloth

https://doi.org/10.1021/acscatal.4c07033
ACS Catal. 2025, 15, 4560−4569

electrode were used as the cathode and anode, respectively. The cathode side was supplied with 20 sccm of an O_2 gas feed rate. The anode side was cycled with DI water. The measured potentials using a two-electrode solid-electrolyte cell setup were not *iR* compensated.

The generated H_2O_2 concentration $C_{titration}$ was evaluated using a standard potassium permanganate (0.1 N $KMnO_4$ solution, Sigma-Aldrich) titration process, according to the following equation

$$5H_2O_2 + 2KMnO_4 + 3H_2SO_4 \rightarrow 5O_2 + 2MnSO_4 + K_2SO_4 + 8H_2O \quad (2)$$

Theoretical concentration that the cell can generate if the FE is 100% is given by

$$C_{theory} = \frac{I}{2 \times 96485 \times L} \quad (3)$$

where I is the current applied, and L is the electrolyte/DI water flow rate in the cell system. Then, the selectivity of H_2O_2 can be calculated as follows

$$\text{FE of } H_2O_2\ (\%) = 100 \times \frac{C_{titration}}{C_{theory}} \quad (4)$$

■ ASSOCIATED CONTENT

Supporting Information

The Supporting Information is available free of charge at https://pubs.acs.org/doi/10.1021/acscatal.4c07033.

Catalyst electrochemical characterization (LSV and ECSA), COMSOL concentration plots, additional membrane and catalyst characterization before and after long-term operation (SEM, BET, and FTIR), and TEA (PDF)

■ AUTHOR INFORMATION

Corresponding Author

Haotian Wang − *Department of Chemical and Biomolecular Engineering, Rice University, Houston, Texas 77005, United States; Department of Chemistry and Department of Materials Science and NanoEngineering, Rice University, Houston, Texas 77005, United States;* orcid.org/0000-0002-3552-8978; Email: htwang@rice.edu

Authors

Yang Xia − *Department of Chemical and Biomolecular Engineering, Rice University, Houston, Texas 77005, United States;* orcid.org/0000-0003-3559-9853

Peng Zhu − *Department of Chemical and Biomolecular Engineering, Rice University, Houston, Texas 77005, United States;* orcid.org/0000-0002-8855-0335

Yile Yang − *Department of Chemical and Biomolecular Engineering, Rice University, Houston, Texas 77005, United States*

Chang Qiu − *Department of Chemical and Biomolecular Engineering, Rice University, Houston, Texas 77005, United States;* orcid.org/0000-0001-5462-7157

Complete contact information is available at: https://pubs.acs.org/10.1021/acscatal.4c07033

Author Contributions

Y.X. and H.W. conceptualized the project. H.W. supervised the project. Y.X. developed and performed catalyst synthesis and conducted the catalytic tests of catalysts and the related data processing. Y.X. performed material characterization. P.Z. performed the techno-economic analysis. Y.Y. performed COMSOL simulations. C.Q. performed electrochemical characterization tests. Y.X. and H.W. wrote the paper. All authors discussed the results and commented on the paper.

Notes

The authors declare no competing financial interest.

■ ACKNOWLEDGMENTS

This work was supported by the David and Lucile Packard Foundation (grant no. 2020-71371) and the Welch Foundation Research grant (C-2051-20230405).

■ REFERENCES

(1) Myers, R. L. *The 100 Most Important Chemical Compounds: A Reference Guide*; Bloomsbury Publishing USA, 2007.

(2) Campos-Martin, J. M.; Blanco-Brieva, G.; Fierro, J. L. Hydrogen peroxide synthesis: an outlook beyond the anthraquinone process. *Angew. Chem., Int. Ed.* **2006**, *45*, 6962−6984.

(3) Perry, S. C.; Pangotra, D.; Vieira, L.; Csepei, L. I.; Sieber, V.; Wang, L.; Ponce de León, C.; Walsh, F. C. Electrochemical synthesis of hydrogen peroxide from water and oxygen. *Nat. Rev. Chem* **2019**, *3*, 442−458.

(4) Goor, G.; Glenneberg, J.; Jacobi, S. *Ullmann's Encyclopedia of Industrial Chemistry*; Wiley, 2020.

(5) Hydrogen peroxide: production costs? https://thundersaidenergy.com/downloads/hydrogen-peroxide-production-costs/(accessed October 12, 2024).

(6) Mekes, J. J. Sustainability and supply chain challenges in hydrogen peroxide. https://www.hpnow.eu/sustainability-and-supply-chain-challenges-in-hydrogen-peroxide/(accessed November 8, 2024).

(7) Ingle, A. A.; Ansari, S. Z.; Shende, D. Z.; Wasewar, K. L.; Pandit, A. B. Progress and prospective of heterogeneous catalysts for H2O2 production via anthraquinone process. *Environ. Sci. Pollut. Res.* **2022**, *29*, 86468−86484.

(8) Yang, S.; Verdaguer-Casadevall, A.; et al. Toward the decentralized electrochemical production of H_2O_2: a focus on the catalysis. *ACS Catal.* **2018**, *8*, 4064−4081.

(9) Jiang, Y.; Ni, P.; Chen, C.; Lu, Y.; Yang, P.; Kong, B.; Fisher, A.; Wang, X. Selective electrochemical H_2O_2 production through two-electron oxygen electrochemistry. *Adv. Energy Mater.* **2018**, *8*, 1801909.

(10) Siahrostami, S.; Verdaguer-Casadevall, A.; et al. Enabling direct H_2O_2 production through rational electrocatalyst design. *Nat. Mater.* **2013**, *12*, 1137−1143.

(11) Lu, Z.; Chen, G.; et al. High-efficiency oxygen reduction to hydrogen peroxide catalysed by oxidized carbon materials. *Nat. Catal.* **2018**, *1*, 156−162.

(12) Kim, H. W.; Ross, M.; et al. Efficient hydrogen peroxide generation using reduced graphene oxide-based oxygen reduction electrocatalysts. *Nat. Catal.* **2018**, *1*, 282−290.

(13) Jiang, K.; Back, S.; Akey, A. J.; Xia, C.; Hu, Y.; Liang, W.; Schaak, D.; Stavitski, E.; Nørskov, J. K.; Siahrostami, S.; et al. Highly selective oxygen reduction to hydrogen peroxide on transition metal single atom coordination. *Nat. Commun.* **2019**, *10*, 3997.

(14) Chen, S.; Chen, Z.; et al. Designing boron nitride islands in carbon materials for efficient electrochemical synthesis of hydrogen peroxide. *J. Am. Chem. Soc.* **2018**, *140*, 7851−7859.

(15) Gao, J.; Yang, H.; et al. Enabling direct H_2O_2 production in acidic media through rational design of transition metal single atom catalyst. *Chem* **2020**, *6*, 658−674.

(16) Zhang, X.; Xia, Y.; Xia, C.; Wang, H. Insights into practical-scale electrochemical H_2O_2 synthesis. *Trends Chem.* **2020**, *2*, 942−953.

(17) Li, Y.; Zhang, Y.; Xia, G.; Zhan, J.; Yu, G.; Wang, Y. Evaluation of the technoeconomic feasibility of electrochemical hydrogen peroxide production for decentralized water treatment. *Front. Environ. Sci. Eng.* **2021**, *15*, 1.
(18) Jiang, Q.; Ji, Y.; Zheng, T.; Li, X.; Xia, C. The Nexus of Innovation: Electrochemically Synthesizing H2O2 and Its Integration with Downstream Reactions. *ACS Mater. Au* **2024**, *4*, 133−147.
(19) Yang, J.; Ding, R.; et al. Optimal MEA structure and operating conditions for fuel cell reactors with hydrogen peroxide and power cogeneration. *J. Phys.: Energy* **2024**, *6*, 015022.
(20) Li, W.; Bonakdarpour, A.; Gyenge, E.; Wilkinson, D. P. Drinking Water Purification by Electrosynthesis of Hydrogen Peroxide in a Power-Producing PEM Fuel Cell. *ChemSusChem* **2013**, *6*, 2137−2143.
(21) Li, W.; Bonakdarpour, A.; Gyenge, E.; Wilkinson, D. P. Production of hydrogen peroxide for drinking water treatment in a proton exchange membrane electrolyzer at near-neutral pH. *J. Electrochem. Soc.* **2020**, *167*, 044502.
(22) Verdaguer-Casadevall, A.; Deiana, D.; et al. Trends in the electrochemical synthesis of H_2O_2: enhancing activity and selectivity by electrocatalytic site engineering. *Nano Lett.* **2014**, *14*, 1603−1608.
(23) Zhang, X.; Zhao, X.; Zhu, P.; Adler, Z.; Wu, Z. Y.; Liu, Y.; Wang, H. Electrochemical oxygen reduction to hydrogen peroxide at practical rates in strong acidic media. *Nat. Commun.* **2022**, *13*, 2880.
(24) Xia, C.; Xia, Y.; Zhu, P.; Fan, L.; Wang, H. Direct electrosynthesis of pure aqueous H_2O_2 solutions up to 20% by weight using a solid electrolyte. *Science* **2019**, *366*, 226−231.
(25) Xia, Y.; Zhao, X.; Xia, C.; Wu, Z. Y.; Zhu, P.; Kim, J. Y.; Bai, X.; Gao, G.; Hu, Y.; Zhong, J.; et al. Highly active and selective oxygen reduction to H_2O_2 on boron-doped carbon for high production rates. *Nat. Commun.* **2021**, *12*, 4225.
(26) Li, H.; Wen, P.; Itanze, D. S.; Hood, Z. D.; Adhikari, S.; Lu, C.; Ma, X.; Dun, C.; Jiang, L.; Carroll, D. L.; et al. Scalable neutral H_2O_2 electrosynthesis by platinum diphosphide nanocrystals by regulating oxygen reduction reaction pathways. *Nat. Commun.* **2020**, *11*, 3928.
(27) Yang, Z.; Ran, J.; Wu, B.; Wu, L.; Xu, T. Stability challenge in anion exchange membrane for fuel cells. *Curr. Opin. Chem. Eng.* **2016**, *12*, 22−30.
(28) Mustain, W. E.; Chatenet, M.; Page, M.; Kim, Y. S. Durability challenges of anion exchange membrane fuel cells. *Energy Environ. Sci.* **2020**, *13*, 2805−2838.
(29) Pantea, D.; Darmstadt, H.; Kaliaguine, S.; Roy, C. Electrical conductivity of conductive carbon blacks: influence of surface chemistry and topology. *Appl. Surf. Sci.* **2003**, *217*, 181−193.
(30) Wang, F.; Kahol, P.; Gupta, R.; Li, X. Experimental studies of carbon electrodes with various surface area for Li−O2 batteries. *J. Electrochem. Energy Convers. Storage* **2019**, *16*, 041007.
(31) Guo, D.; Shibuya, R.; Akiba, C.; et al. Active Sites of Nitrogen-Doped Carbon Materials for Oxygen Reduction Reaction Clarified Using Model Catalysts. *Science* **2016**, *351* (6271), 361−365.
(32) Jia, Y.; Dastafkan, K.; Ren, W.; Yang, W.; Zhao, C. Carbon-Based Catalysts for Electrochemical CO_2 Reduction. *Sustainable Energy Fuels* **2019**, *3*, 2890−2906.
(33) Zhu, P.; Wu, Z.; et al. Continuous carbon capture in an electrochemical solid-electrolyte reactor. *Nature* **2023**, *618*, 959−966.
(34) DOE Hydrogen and Fuel Cells Program Record 19009. https://www.hydrogen.energy.gov/docs/hydrogenprogramlibraries/pdfs/19009_h2_production_cost_pem_electrolysis_2019.pdf?Status=Master (accessed June 11, 2024).

https://doi.org/10.1021/acscatal.4c07033
ACS Catal. 2025, 15, 4560−4569